

Banner appropriate to article type will appear here in typeset article

Revisiting the hydrodynamic modulation of short surface waves by longer waves

Milan Curcic¹†

¹Rosenstiel School of Marine, Atmospheric, and Earth Science, University of Miami, Miami, FL

²Frost Institute for Data Science and Computing, University of Miami, Coral Gables, FL

(Received xx; revised xx; accepted xx)

Hydrodynamic modulation of short ocean surface waves by longer ambient waves significantly influences remote sensing, interpretation of *in situ* wave measurements, and numerical wave forecasting. This paper revisits the wave crest and action conservation laws and derives steady, nonlinear, analytical solutions for the change of short-wave wavenumber, action, and gravitational acceleration due to the presence of longer waves. We validate the analytical solutions with numerical simulations of the full conservation equations. The nonlinear analytical solutions of short-wave wavenumber, amplitude, and steepness modulation significantly deviate from the linear analytical solutions of Longuet-Higgins & Stewart (1960), and are similar to the nonlinear numerical solutions by Longuet-Higgins (1987) and Zhang & Melville (1990). The short-wave steepness modulation is attributed 5/8 to wavenumber, 1/4 due to wave action, and 1/8 due to effective gravity. Examining the homogeneity and stationarity requirements for the conservation of wave action reveals that stationarity is a stronger requirement and is generally not satisfied for very steep long waves. We examine the results of Peureux *et al.* (2021) who found through numerical simulations that the short-wave modulation grows unsteadily with each long-wave passage. We show that this unsteady growth only occurs for homogeneous initial conditions as a special case and not generally. The proposed steady solutions are a good approximation of the nonlinear crest-action conservation solutions in long-wave steepness $\lesssim 0.2$. Except for a subset of initial conditions, the solutions to the non-linearised crest-action conservation equations are mostly steady in the reference frame of the long waves.

Key words:

1. Introduction

Short ocean surface waves are hydrodynamically modulated by longer swell. As long waves propagate through a field of shorter waves, their orbital velocities cause near-surface convergence and divergence on the front and rear faces of the long waves, respectively. Following Unna (1941, 1942, 1947), Longuet-Higgins & Stewart (1960) introduced a steady, approximate solution for hydrodynamic modulation of short waves by longer waves:

† Email address for correspondence: mcurcic@miami.edu

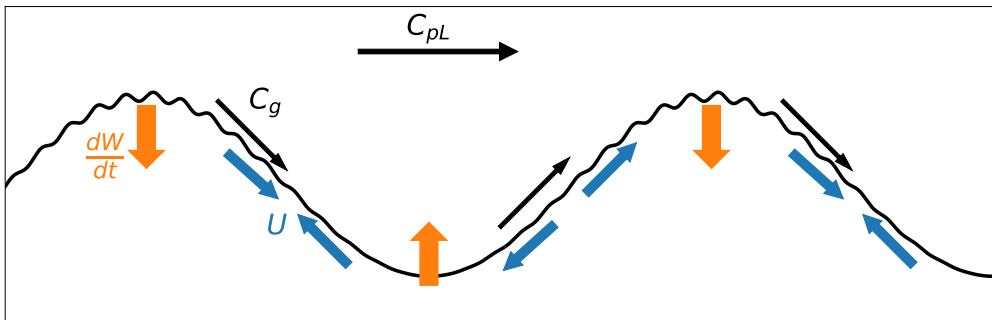


Figure 1: A diagram of short waves riding on longer waves that propagate with their phase-speed C_{pL} from left to right. The short waves propagate on the long-wave surface, their action moving with the group velocity C_g . Long waves induce orbital velocities U that cause near-surface convergence and divergence on their front and rear faces, respectively. They also induce downward and upward centripetal accelerations (dW/dt) in the crests and troughs, respectively, that modulate the effective gravity at the surface. As a consequence of surface convergence and divergence and the effective-gravity modulation, the short waves become shorter and higher preferentially on the long-wave crests. The diagram is not to scale.

$$\tilde{k} = k(1 + \varepsilon_L \cos \psi) \quad (1.1)$$

where \tilde{k} and k are the modulated and unmodulated short-wave wavenumbers, respectively, $\varepsilon_L = a_L k_L$ is the steepness of the long wave with wavenumber k_L and amplitude a_L , and ψ is the long-wave phase. This process is illustrated in Fig. 1. Hydrodynamic modulation is a key process for the development and interpretation of remote sensing of ocean surface waves and currents (Keller & Wright 1975; Alpers & Hasselmann 1978; Hara & Plant 1994) and is distinguished from aerodynamic modulation (Donelan 1987; Belcher 1999; Chen & Belcher 2000). Experimental studies of the general short-wave modulation problem included both the laboratory (e.g., Keller & Wright 1975; Donelan *et al.* 2010) and field (e.g., Hara *et al.* 2003; Plant 1977) measurements. Phillips (1981) and Longuet-Higgins (1987) revisited the hydrodynamic modulation problem by considering nonlinear long waves and variations in the effective gravity of short waves. Their results yielded significantly stronger modulation than previously predicted by Longuet-Higgins & Stewart (1960). Henyey *et al.* (1988) derived an analytical solution for the modulation of short waves using Hamiltonian mechanics and reported similar modulation magnitudes to that of Longuet-Higgins (1987). Zhang & Melville (1990) considered weakly nonlinear short waves using a nonlinear Schrödinger equation and found stronger wavenumber modulation but weaker amplitude modulation than those predicted by Longuet-Higgins (1987). Aside from the early linear solutions by Longuet-Higgins & Stewart (1960), the variety of analytical and numerical frameworks (Eulerian crest and action conservation, Hamiltonian, Schrödinger) that tackle the same fundamental physics and that relatively closely reproduce the steady solutions for short-wave modulation suggests that the solutions are robust. Nevertheless, alternative analytical and numerical approaches to the modulation problem remain of interest, especially if higher degrees of nonlinearity can be considered using simpler approaches.

All modulation solutions mentioned thus far are steady in the reference frame of the long wave—short waves become shorter and higher (and thus, steeper) preferentially on the long-wave crests. Conversely, they elongate and flatten preferentially in the long-wave troughs. Recently, Peureux *et al.* (2021) asked whether the steady (*i.e.*, stationary; not

Reference	Analysis framework	Solution type	Solution steadiness	Nonlinear long waves	Nonlinear short waves
Longuet-Higgins & Stewart (1960)	Velocity potential	Analytical	Steady	No	No
Phillips (1981)	Crest and action conservation	Numerical	Steady	Yes	No
Longuet-Higgins (1987)	Crest and action conservation	Numerical	Steady	Yes	No
Henye <i>et al.</i> (1988)	Hamiltonian	Analytical	Steady	Yes	No
Zhang & Melville (1990)	Schrödinger	Numerical	Steady	Yes	Yes
Peureux <i>et al.</i> (2021)	Crest and action conservation	Numerical	Unsteady	No	No
This paper	Crest and action conservation	Analytical and numerical	Steady and unsteady	Yes	No

Table 1: Non-exhaustive summary of prior and present (this paper) approaches to calculating the modulation of short waves by long waves. The solution steadiness refers to whether the solution depends on time (unsteady) or not (steady).

depending on time) solutions of short-wave modulation are appropriate by simulating the full wave conservation equations. They found that the short waves grow unsteadily due to the propagation of longer waves, suggesting that the steady-state solutions may only be valid for a few long-wave periods before the short waves begin to break due to excessive steepness. However, the unsteadiness of their solutions occurs in a specific scenario in which a long-wave train suddenly appears to modulate a uniform field of short waves. The numerical simulations stabilise if the short-wave field is initialised from existing steady solutions, like those by Longuet-Higgins & Stewart (1960). Nevertheless, their results do put into question whether the short-wave modulation predicted by theory is generally steady over many long-wave periods or not. Looking at the conservation equations alone, it is not obvious that it is.

In this paper, we revisit this problem from the perspective of wave action conservation but consider the long-wave slope to be significant enough to require evaluating the short-waves at the long-wave surface rather than at the mean water level. This allows us to derive alternative, steady, nonlinear solutions for the modulation of short waves, within the limits of small ε_L . The analytical solutions yield modulations that are stronger than the original solution by Longuet-Higgins & Stewart (1960), but similar to the nonlinear numerical solutions by Longuet-Higgins (1987) and Zhang & Melville (1990) for $\varepsilon_L \lesssim 0.2$. To validate the steadiness of the analytical solutions, we perform numerical simulations of the full wave crest and action conservation laws, and compare the results to the analytical solutions presented here, as well as the prior numerical results. The numerical simulations are used to determine the validity of the approximate steady solution and to investigate the unsteadiness of the short-wave modulation found by Peureux *et al.* (2021). The main

prior studies on hydrodynamic modulation, and their assumptions and approaches to the solution, are summarised in Table 1. We first present the governing equations in §2, and then the analytical solutions for the modulation of short waves by long waves in §3. Then, we describe the numerical simulations and their results in §4. Finally, we discuss the results and their implications in §5 and conclude the paper in §6.

2. Governing equations

The flow is inviscid, irrotational, and incompressible, and without sources or sinks. In these conditions, linear, deep-water, surface gravity waves obey the dispersion relation:

$$\omega = \sqrt{gk} + kU \quad (2.1)$$

where ω is the angular frequency in a fixed reference frame, g is the gravitational acceleration, k is the wavenumber, and U is the mean advective current in the direction of the wave propagation. A current in the direction of the waves increases their absolute frequency without changing their wavenumber. An important limitation here is that U must be slowly varying on the scales of the wave period (Bretherton & Garrett 1968). From the perspective of short waves riding on long waves, the advective current is the horizontal near-surface orbital velocity of the long wave. Strictly, a velocity profile must be considered when determining the advective velocity for a wave of any given wavenumber (Stewart & Joy 1974), however, for brevity, here we will assume a surface velocity to be the advective one for short waves. The evolution of the short-wave wavenumber is described by the conservation of wave crests (e.g., Whitham 1974; Phillips 1981):

$$\frac{\partial k}{\partial t} + \frac{\partial \omega}{\partial x} = 0 \quad (2.2)$$

where t and x are time and space, respectively. This relation states that the wavenumber must change locally when the frequency varies in space.

(2.1) and (2.2) describe the evolution of the short-wave wavenumber. To describe the evolution of the wave amplitude, use the wave action balance (Bretherton & Garrett 1968) in absence of sources (e.g. due to wind) and sinks (e.g. due to whitecapping):

$$\frac{\partial N}{\partial t} + \frac{\partial}{\partial x} [(C_g + U) N] = 0 \quad (2.3)$$

where N is the action of short waves defined as the ratio of their energy to their intrinsic frequency, E/σ , and $C_g = 1/2\sqrt{g/k}$ is their group speed in deep water. The wave action expressed as E/σ is commonly taken as conservative in wave modulation theory (Phillips 1981; Longuet-Higgins 1987), however as Dysthe *et al.* (1988) show, it is conservative only for gently sloped waves. We describe this and other requirements in more detail further below and show in what long-wave conditions they are satisfied. The wave crest conservation (2.2) follows from the assumption of a conserved wave phase, which is limited by the same set of requirements as those for the wave action conservation (e.g., Whitham 1974). Although the absence of wave growth and dissipation is not generally realistic in the open ocean, it is a useful approximation here to isolate the effects of hydrodynamic modulation solely due to the motion of the long waves.

Short waves that ride on the surface of the longer waves move in an accelerated reference frame (due to the centripetal acceleration at the long-wave surface) and thus experience effective gravitational acceleration that varies in space and time (Phillips 1981; Longuet-Higgins 1986, 1987). Inserting (2.1) into (2.2) and noting that:

$$\frac{\partial \sqrt{gk}}{\partial x} = \frac{1}{2} \sqrt{\frac{g}{k}} \frac{\partial k}{\partial x} + \frac{1}{2} \sqrt{\frac{k}{g}} \frac{\partial g}{\partial x} \quad (2.4)$$

we get:

$$\frac{\partial k}{\partial t} + (C_g + U) \frac{\partial k}{\partial x} + k \frac{\partial U}{\partial x} + \frac{1}{2} \sqrt{\frac{k}{g}} \frac{\partial g}{\partial x} = 0 \quad (2.5)$$

From left to right, the terms in this equation represent the change in wavenumber due to the propagation and advection by ambient current U , the convergence of the ambient current, and the spatial inhomogeneity of the gravitational acceleration. In a non-accelerated reference frame (i.e. in absence of longer waves), the last term vanishes. It is otherwise necessary to conserve the wave crests.

For the wave action, expand (2.3) to get:

$$\frac{\partial N}{\partial t} + (C_g + U) \frac{\partial N}{\partial x} + N \frac{\partial U}{\partial x} + N \frac{\partial C_g}{\partial x} = 0 \quad (2.6)$$

This equation is similar to (2.5), except for the last term which represents the inhomogeneity of the group speed. As Peureux *et al.* (2021) explained, the presence of this term causes unsteady growth of wave action in infinite long-wave trains. (2.5) and (2.6) are the governing equations that we approximate and solve analytically in §3, and numerically in their full form in §4. This system of equations is semi-coupled, meaning that it is possible to solve (2.5) on its own, but solving (2.6) requires also the solution of (2.5). In other words, the wave kinematics (the wavenumber distribution) are not concerned with the wave action. In contrast, the wave action is governed, among others, by the group velocity and thus depends on the wavenumber.

For the ambient forcing, we consider a train of monochromatic long waves defined, to the first order in ε_L , by the elevation $\eta_L = a_L \cos \psi$, where $\psi = k_L x - \sigma_L t$ is the long-wave phase and σ_L its angular frequency. The velocity potential of the long wave is:

$$\phi = \frac{a_L \omega_L}{k_L} e^{k_L z} \sin \psi + \mathcal{O}(\varepsilon_L^4) \quad (2.7)$$

where z is the vertical distance from the mean water level that is positive upwards. When evaluated at the mean water level ($z = 0$), (2.7) is accurate to the third order in ε_L in deep water because the second- and third-order terms in the Stokes expansion series are exactly zero. The long-wave induced horizontal and vertical orbital velocities are:

$$U = \frac{\partial \phi}{\partial x} = a_L \omega_L e^{k_L z} \cos \psi + \mathcal{O}(\varepsilon_L^4) \quad (2.8)$$

$$W = \frac{\partial \phi}{\partial z} = a_L \omega_L e^{k_L z} \sin \psi + \mathcal{O}(\varepsilon_L^4) \quad (2.9)$$

Evaluating these velocities at the wave surface $z = \eta_L$ rather than at the mean water level $z = 0$ is a departure from the linear theory, making the treatment of the long waves here as weakly nonlinear. As Zhang & Melville (1990) point out, this is appropriate to do when the amplitude of the long waves is of the similar magnitude or larger than the wavelength of the short waves. However, evaluating these velocities at the free surface $z = \eta_L$ introduces an additional error of $\mathcal{O}(\varepsilon_L^2)$. The surface velocity errors are described in more detail in Appendix A.

(2.5)-(2.6) are the governing equations used in this paper, with (2.8)-(2.9) describing the long-wave induced ambient velocity forcing for the short waves. Rather than deriving the modulation solution from the velocity potential of two waves, as Longuet-Higgins & Stewart (1960) did, starting from the crest-action conservation balances allows for a simpler derivation.

3. Analytical solutions

We now describe the analytical solutions for the short-wave wavenumber, effective gravitational acceleration, amplitude, and steepness in the presence of long waves. The wavenumber is derived by linearising the conservation of wave crests (2.2) and neglecting the spatial gradients of k and g . The effective gravity is derived by projecting the long-wave induced surface accelerations onto the local vertical axis (that is, the axis normal to the long-wave surface), akin to Zhang & Melville (1990). The amplitude is derived by first evaluating the short-wave action from the action conservation (2.3) and then applying the modulated effective gravity to obtain the amplitude. From the modulated wavenumber, amplitude, and effective gravity, the steepness, frequency, and phase speed readily follow from the usual wave relationships. Going forward we will use the tilde over the variables to denote the modulated quantities (e.g. \tilde{k} for wavenumber).

3.1. Wavenumber modulation

Solving analytically for the wavenumber requires dropping the spatial derivatives of k in (2.5) and assuming homogeneous g :

$$\frac{\partial k}{\partial t} = -k \frac{\partial U}{\partial x} \quad (3.1)$$

Although Peureux *et al.* (2021) pointed out that the solution by Longuet-Higgins & Stewart (1960) requires assuming homogeneous group speed of the short-wave field, in fact, it also requires assuming no horizontal propagation and advection of the short waves. Combine (2.8) and (3.1) and integrate in time to get:

$$\frac{\tilde{k}}{k} = e^{\varepsilon_L \cos \psi} e^{\varepsilon_L \cos \psi} \quad (3.2)$$

Notice that the Taylor expansion of (3.2) to the first order recovers the original solution by Longuet-Higgins & Stewart (1960):

$$\frac{\tilde{k}}{k} = 1 + \varepsilon_L \cos \psi \quad (3.3)$$

Coming from the conservation of crests, as opposed to the velocity potential superposition, the solution by Longuet-Higgins & Stewart (1960) requires two approximations: First, evaluating the long-wave velocity at $z = 0$ rather than $z = \eta_L$; and second, truncating the Taylor expansion series beyond $\mathcal{O}(\varepsilon_L)$. These approximations underestimate the short-wave modulation magnitude (Fig. 2). At the wave crest, (3.2) yields the wavenumber modulation that is 16.9%, 38.5%, 66.4%, and 104% larger than that of Longuet-Higgins & Stewart (1960) for $\varepsilon_L = 0.1, 0.2, 0.3, 0.4$, respectively. Although not immediately obvious from the expressions, the modulated wavenumber (3.3) is conserved across the long-wave phase, whereas the higher-order solution (3.2) is not. This is because combining the orbital velocities evaluated at $z = \eta_L$ and the linearised conservation of wave crests in (2.5) creates excess short-wave wavenumber. The solution of (2.5) must be conservative across the long-wave

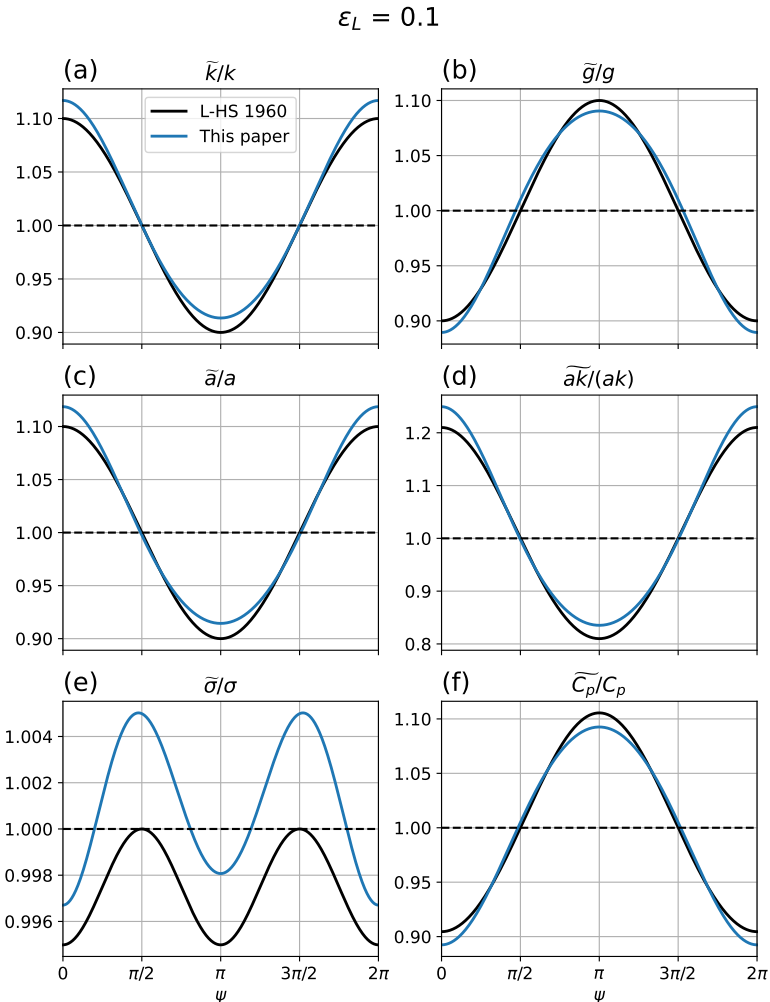


Figure 2: Steady analytical solutions for the modulation of short-wave (a) wavenumber, (b) gravitational acceleration, (c) amplitude, (d) steepness, (e) intrinsic frequency, and (f) intrinsic phase speed as function of long-wave phase for $\varepsilon_L = 0.1$, based on Longuet-Higgins & Stewart (1960) (L-HS 1960, black) and this paper (blue). Long-wave crest and trough are located at $\psi = 0$ and $\psi = \pi$, respectively.

phase, as we will see later from the numerical simulations. The steady analytical solutions for modulation of short-wave effective gravity, amplitude, steepness, intrinsic frequency, and phase speed are also shown in Fig. 2, for reference, however, their formulations appear in the following subsections. Although the analytical solutions by Longuet-Higgins & Stewart (1960) have been updated by the numerical results of Longuet-Higgins (1987), they are here nevertheless relevant to use as reference for the proposed analytical solutions. This comparison allows quantifying solely the effect of evaluating the long-wave properties at the surface rather than at the mean water level.

3.2. Gravity modulation

Three distinct effects contribute to the modulation of the effective gravity of short waves in the presence of long waves. First, long waves induce orbital (centripetal) accelerations

on their surface, so the short waves ride in an accelerated reference frame and experience effective gravity that is lower at the crests and higher in the troughs (Longuet-Higgins 1986, 1987). This is an $O(\varepsilon_L)$ effect. Second, it is important to distinguish between the Eulerian and Lagrangian effective gravities (Longuet-Higgins 1986). The Eulerian gravity is that which would be measured by a fixed wave staff, for example, and features sharp and strong minima at the crests and broad and weak maxima in the troughs. In contrast, the Lagrangian gravity is that which is experienced by a short wave group that propagates with its own group speed and is advected by the ambient, long-wave induced, velocity. The Lagrangian velocity is overall smoother and more attenuated compared to its Eulerian counterpart because the local slope as experienced by the travelling short-wave group is gentler. The two gravities are related by:

$$\tilde{g}_l = g + \frac{dW}{dt} = g + \frac{\partial W}{\partial t} + (C_g + U) \frac{\partial W}{\partial x} = \tilde{g}_e + (C_g + U) \frac{\partial W}{\partial x} \quad (3.4)$$

where l and e subscripts serve to denote "Lagrangian" and "Eulerian", respectively. Although Longuet-Higgins (1986) thoroughly described the differences between the Eulerian and Lagrangian effective gravities, he did so for a fully-nonlinear irrotational gravity wave, which can be computed numerically but not analytically. Note also that when evaluating the Lagrangian effective gravity, Longuet-Higgins (1987) considered the orbital motion of the long wave but not the propagation speed of the short-wave group, which can exceed the ambient velocity U depending on the properties of the short and long waves considered. Group speed of the short waves aside, the Lagrangian correction to the gravity being an advective term is $O(\varepsilon_L^2)$. Third, the projection of the long-wave induced horizontal acceleration in the curvilinear coordinate system contributes small but non-negligible effects on the short-wave effective gravity (Phillips 1981; Zhang & Melville 1990). These three effects are completely described by projecting the gravitational acceleration vector from the coordinate that is perpendicular to the mean water surface ($z = 0$) to that which is perpendicular to the long-wave surface ($z = \eta_L$), and likewise for the long-wave orbital accelerations:

$$\frac{\tilde{g}}{g} = \cos \alpha + \frac{1}{g} \frac{dW_{z=\eta_L}}{dt} \cos \alpha + \frac{1}{g} \frac{dU_{z=\eta_L}}{dt} \sin \alpha \quad (3.5)$$

$$\alpha = \tan^{-1} \frac{\partial \eta}{\partial x} \quad (3.6)$$

where α is the local slope of the long-wave surface. For short waves on a linear long wave, the Eulerian gravity modulation is:

$$\frac{\tilde{g}_e}{g} = \frac{1 - \varepsilon_L \cos \psi e^{\varepsilon_L \cos \psi} [1 + (\varepsilon_L \sin \psi)^2 e^{\varepsilon_L \cos \psi}]}{\sqrt{(\varepsilon_L \sin \psi)^2 + 1}} \quad (3.7)$$

The same derivation can be carried out for the Lagrangian gravity modulation following (3.4)-(3.6), and is omitted here for brevity. Curvilinear effects on effective gravity can be removed altogether by setting $\alpha = 0$. In that case, (3.7) simplifies to:

$$\frac{\tilde{g}_e}{g} = 1 - \varepsilon_L \cos \psi e^{\varepsilon_L \cos \psi} \quad (3.8)$$

If we evaluate the orbital accelerations at the mean water level $z = 0$, this further simplifies to:

$$\frac{\tilde{g}_e}{g} = 1 - \varepsilon_L \cos \psi \quad (3.9)$$

which is the form used by Longuet-Higgins & Stewart (1960) and Peureux *et al.* (2021), for example. The Lagrangian correction in (3.4) is:

$$U \frac{\partial W}{\partial x} = g \varepsilon_L^2 \cos^2 \psi e^{2\varepsilon_L \cos \psi} + \mathcal{O}(\varepsilon_L^3) \quad (3.10)$$

and so it becomes important only for large ε_L .

The general form of the gravity modulation (3.5) is convenient because it allows us to easily attribute the modulation to different processes. It also makes it straightforward to evaluate the gravity modulation for different long-wave forms, by evaluating the orbital accelerations and the local slope for each wave form. For a third-order Stokes wave, for example, the elevation is:

$$\eta_{St} = a_L \left[\cos \psi + \frac{1}{2} \varepsilon_L \cos 2\psi + \varepsilon_L^2 \left(\frac{3}{8} \cos 3\psi - \frac{1}{16} \cos \psi \right) \right] + \mathcal{O}(\varepsilon_L^4) \quad (3.11)$$

Without considering the curvilinear effects in (3.5), the gravitational acceleration at the surface of a Stokes wave is, to the third order:

$$\frac{\tilde{g}}{g} = \left\{ 1 - \varepsilon_L e^{k\eta_{St}} \left[\cos \psi - \varepsilon_L \sin \psi \left(\sin \psi + \varepsilon_L \sin 2\psi - \frac{1}{16} \varepsilon_L^2 \sin \psi + \frac{9}{8} \varepsilon_L^2 \sin 3\psi \right) \right] \right\} \quad (3.12)$$

The equivalent expression that includes the curvilinear effects can be derived by evaluating the velocities and the local slope α at $z = \eta_{St}$, and inserting them into (3.5):

$$\frac{\tilde{g}}{g} = \cos \alpha_{St} + \frac{dW_{z=\eta_{St}}}{dt} \cos \alpha_{St} + \frac{dU_{z=\eta_{St}}}{dt} \sin \alpha_{St} \quad (3.13)$$

$$\alpha_{St} = \tan^{-1} \frac{\partial \eta_{St}}{\partial x} \quad (3.14)$$

Let us now examine the contributions of the different terms to the short-wave effective gravity modulation. Fig. 3a shows the effective gravity modulation of short waves as a function of the long-wave phase for $\varepsilon_L = 0.3$, for a variety of the gravity modulation forms. Although quite steep, this value of ε_L allows easier visualisation of the modulation differences. To $\mathcal{O}(\varepsilon_L)$, the gravity modulation is out of phase with the long-wave elevation, with the short waves experiencing a lower effective gravity on the long-wave crests and a higher effective gravity in the troughs. Evaluating the orbital accelerations at $z = \eta$ and the Lagrangian gravity correction each have an $\mathcal{O}(\varepsilon_L^2)$ contribution but of opposite signs. The former amplifies the gravity modulation while the latter attenuates it. The curvilinear effects are significant at the front and rear faces of the long wave but not near the crests and troughs. The long-wave surface slope has a $\mathcal{O}(\varepsilon_L^2)$ effect. Naturally, the slope is exactly zero at the crests and the troughs, and its effects are largest at the front and rear faces of the long wave, where the covariance between the local slope and the horizontal accelerations is largest. Evaluating the velocities and accelerations at the surface of a third-order Stokes wave causes a correction mostly at the faces of the long wave. Finally, numerically computing the surface velocities and accelerations of a fully-nonlinear wave allows us to exclude uncertainties associated with the truncation errors of the Stokes expansion at first and third orders in ε_L . At this steepness,

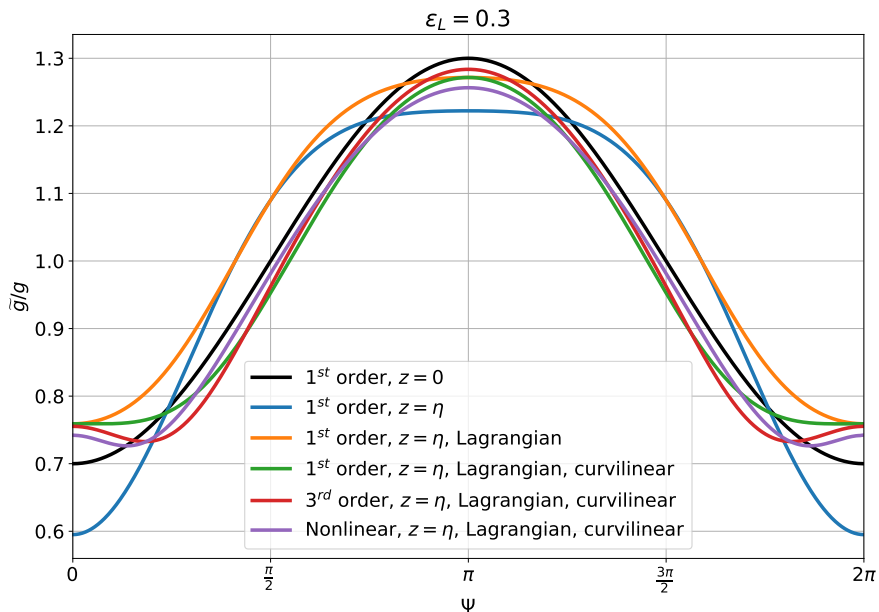


Figure 3: Analytical solutions for the effective gravitational acceleration modulation by long waves, as function of the long-wave phase, for $\varepsilon_L = 0.3$. Black is for Eulerian gravity of a linear wave evaluated at $z = 0$; blue is the same as black but evaluated at $z = \eta$; orange is the same as blue but for Lagrangian gravity; green is the same as orange but in a curvilinear reference frame; red is the same as green but for a third-order Stokes wave; and purple is the same as red but for a fully-nonlinear wave. The elevation and surface velocities for the fully-nonlinear wave are computed following Clamond & Dutykh (2018). Long-wave crest and trough are located at $\psi = 0$ and $\psi = \pi$, respectively.

the fully-nonlinear solution is marginally different from that of the third-order Stokes wave (see also Appendix A for the errors in surface velocity estimates of the linear and third-order Stokes approximations).

It is instructive to also examine the minimum values of the effective gravity as function of long-wave steepness ε_L (Fig. 4), as the minima occur at or near the long-wave crests where the short-wave modulation is largest. Without the Lagrangian correction to the effective gravity, the gravity modulation is overestimated; for accelerations evaluated at the surface of a linear wave, the maximum gravity reduction is 60% at $\varepsilon_L = 0.4$. The Lagrangian correction attenuates the gravity modulation, making the gravity reduction at the crests $\approx 25\%$. As the slope effects on the effective gravity exist only away from crests and troughs, they may be neglected in the steady solutions where modulation is typically evaluated at the long-wave crests. Here, the slope effect causes a difference in the minimum effective gravity for $\varepsilon_L \gtrsim 0.3$. The effective gravity reduction at the crests in the case of a fully-nonlinear wave is $\approx 10\%$, 19% , 27% , and 40% , for ε_L of 0.1, 0.2, 0.3, and 0.4, respectively. These are similar to the fully-nonlinear numerical estimates of Longuet-Higgins (1986, 1987).

3.3. Amplitude and steepness modulation

The modulation of short-wave amplitude can be derived in a similar way as we did for the wavenumber, except that here we linearise the wave action balance (2.6) and integrate it in time:

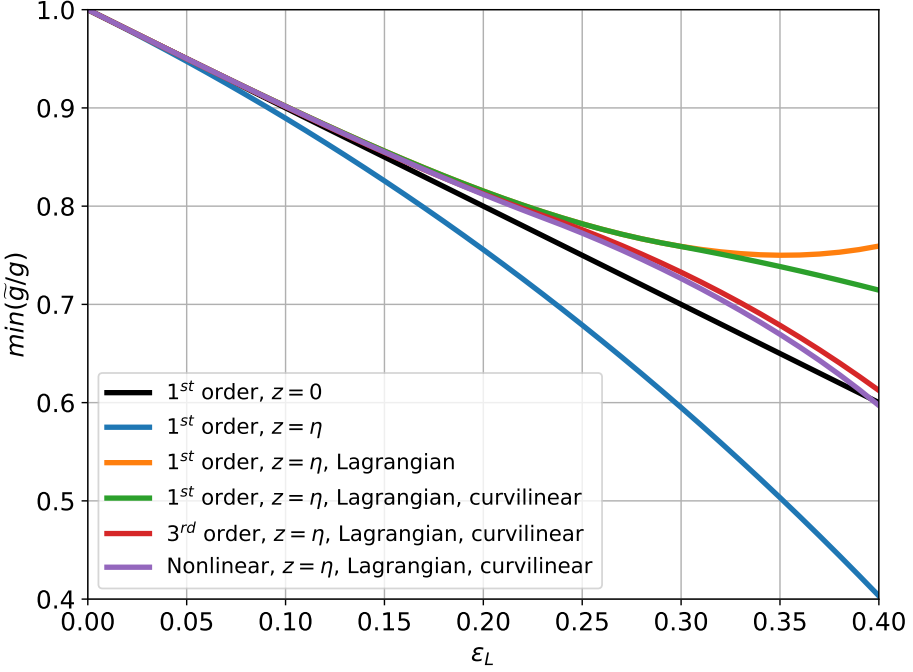


Figure 4: As Fig. 3 but showing the minimum short-wave gravity modulation as function of long-wave steepness ε_L .

$$\frac{\tilde{N}}{N} = e^{\varepsilon_L \cos \psi} e^{\varepsilon_L \cos \psi} \quad (3.15)$$

Since wave action is energy divided by the intrinsic frequency σ , and energy scales with ga^2 , the modulation of the amplitude is related to the modulations of gravity, wavenumber, and action:

$$\frac{\tilde{a}}{a} = \sqrt{\frac{\tilde{g} \tilde{\sigma} \tilde{N}}{\tilde{g} \tilde{\sigma} N}} = \left(\frac{\tilde{k}}{k}\right)^{\frac{1}{4}} \left(\frac{\tilde{N}}{N}\right)^{\frac{1}{2}} \left(\frac{\tilde{g}}{g}\right)^{-\frac{1}{4}} \quad (3.16)$$

To $\mathcal{O}(\varepsilon_L)$, and using (3.2) and (3.15), the above simplifies to the result of Longuet-Higgins & Stewart (1960):

$$\frac{\tilde{a}}{a} = \left(\frac{\tilde{g}}{g}\right)^{-\frac{1}{4}} (1 + \varepsilon_L)^{\frac{3}{4}} \approx \frac{(1 + \varepsilon_L)^{\frac{3}{4}}}{(1 - \varepsilon_L)^{\frac{1}{4}}} \approx 1 + \varepsilon_L \quad (3.17)$$

The amplitude and steepness modulation of the short waves as a function of the long-wave phase for $\varepsilon_L = 0.1$ are compared to the Longuet-Higgins & Stewart (1960) solutions in Fig. 2 panels (c) and (d), respectively. Also shown are the modulation of the short-wave intrinsic frequency and phase speed in panels (e) and (f), respectively. As the wavenumber and gravity modulations are both $\mathcal{O}(\varepsilon_L)$ and out of phase, the intrinsic frequency modulation is $\mathcal{O}(\varepsilon_L^2)$, positive on the long-wave faces and negative on the crests and troughs. For the short-wave

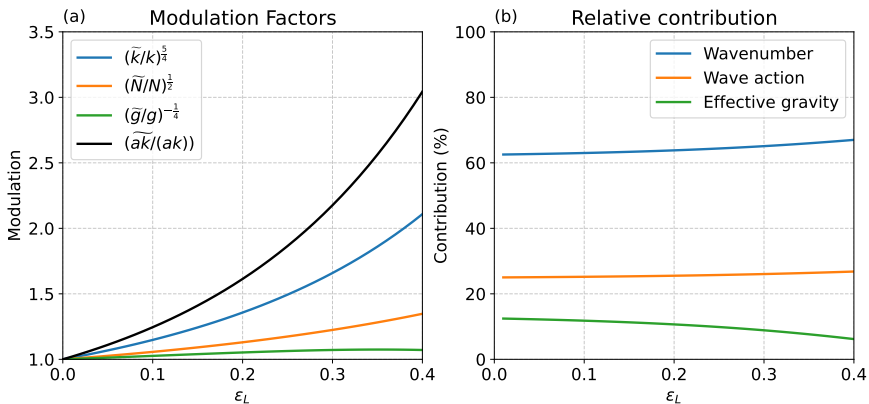


Figure 5: Contributions of short-wave wavenumber, action, and effective gravity modulations to the steepness modulation, as function of the long-wave steepness ε_L . Panel (a) shows each modulation factor (colour) and their product (black), and panel (b) shows their relative contributions in percentage, calculated as the ratio of the logarithm of each modulation factor to the logarithm of the product of all modulations.

phase speed modulation, the wavenumber and gravity modulations work in tandem and cause the short-wave phase speed to be reduced on the long-wave crests and increased in the troughs.

Finally, the short-wave steepness modulation follows from (3.16):

$$\frac{\widetilde{a}k}{ak} = \left(\frac{\widetilde{k}}{k}\right)^{\frac{5}{4}} \left(\frac{\widetilde{N}}{N}\right)^{\frac{1}{2}} \left(\frac{\widetilde{g}}{g}\right)^{-\frac{1}{4}} \quad (3.18)$$

The short-wave steepness modulation at the long-wave crests is thus largely controlled by the wavenumber modulation (5/8, or, 62.5%), followed by the convergence of wave action (1/4, or, 25%), and by least amount by the effective gravity reduction (1/8, or, 12.5%) (Fig. 5). (3.18) and Fig. 5 demonstrate that more than half of the steepness modulation can be captured by the wavenumber modulation alone. Further, considering the wavenumber and wave action modulations, while neglecting the gravity modulation, captures $\approx 88\%$ of the steepness modulation at the long-wave crests. This result may be useful for the interpretation of remote sensing products that resolve some but not all of the short-wave modulation effects. Finally, the relative contributions of different modulation factors remain mostly constant as ε_L increases, with only a mild decrease of the effective gravity modulation contribution, and mild increases of the wavenumber and wave action modulation contributions.

3.4. Limits to the wave action conservation

Following the variational approach by Whitham (1965), Bretherton & Garrett (1968) showed that the wave action is conserved for small-amplitude (linear) waves that propagate in slowly-varying media. Longuet-Higgins (1987) correctly pointed out both requirements—that both the medium and the short wavetrain must be slowly-varying—for the wave action conservation to hold. However, he incorrectly stated that there is no explicit restriction on the steepness of the long wave, and that it appears necessary to only assume small-amplitude short waves and significant scale separation (k/k_L). The restriction on ε_L becomes apparent when we recognize that the long wave-induced orbital velocity scales with ε_L , and that the divergence of this velocity is the dominant term in (2.5) and (2.6). Here we show that in the general

case both the homogeneity and the stationarity of a short wave quantity q depend on the long-wave steepness ε_L .

The homogeneity and stationarity of a scalar quantity q can be expressed as conditions on the instantaneous fractional rate of change of q being much smaller than the short-wave inverse scales:

$$\frac{1}{q} \frac{\partial q}{\partial x} \ll k \quad (3.19)$$

$$\frac{1}{q} \frac{\partial q}{\partial t} \ll \sigma \quad (3.20)$$

The slowly-varying conditions on the medium (in our case, the long-wave orbital velocity U) are then:

$$\frac{1}{U} \frac{\partial U}{\partial x} \ll \tilde{k}, \quad (3.21)$$

$$\frac{1}{U} \frac{\partial U}{\partial t} \ll \tilde{\sigma}, \quad (3.22)$$

respectively. For a linear long wave, these conditions are equivalent to the scale separation between the long and short waves:

$$k_L \ll \tilde{k} \quad (3.23)$$

$$\sigma_L \ll \tilde{\sigma} \quad (3.24)$$

Bretherton & Garrett (1968) also require that the medium is nearly uniform over the vertical scales of motion of the short waves. For the ambient velocity being the orbital velocity of the long wave, this is trivially satisfied with (3.23).

Now, to address the variation of short-wave properties, we apply (3.19)-(3.20) to the long-wave phase dependent wavenumber, gravitational acceleration, and wave action, and define the homogeneity and stationarity as:

$$H_q = 1 - \left| \frac{1}{qk} \frac{\partial q}{\partial x} \right| \quad (3.25)$$

$$S_q = 1 - \left| \frac{1}{q\sigma} \frac{\partial q}{\partial t} \right| \quad (3.26)$$

With the above definitions, we consider q to be homogeneous and stationary as $H_q \rightarrow 1$ and $S_q \rightarrow 1$, respectively.

For the linearised modulation solutions (3.2), (3.9), and (3.15), the respective homogeneity expressions are:

$$H_{k,N} = 1 - \frac{k_L}{k} \left| \frac{\varepsilon_L \sin \psi}{(1 + \varepsilon_L \cos \psi)^2} \right| \quad (3.27)$$

$$H_g = 1 - \frac{k_L}{k} \left| \frac{\varepsilon_L \sin \psi}{(1 - \varepsilon_L^2 \cos^2 \psi)} \right| \quad (3.28)$$

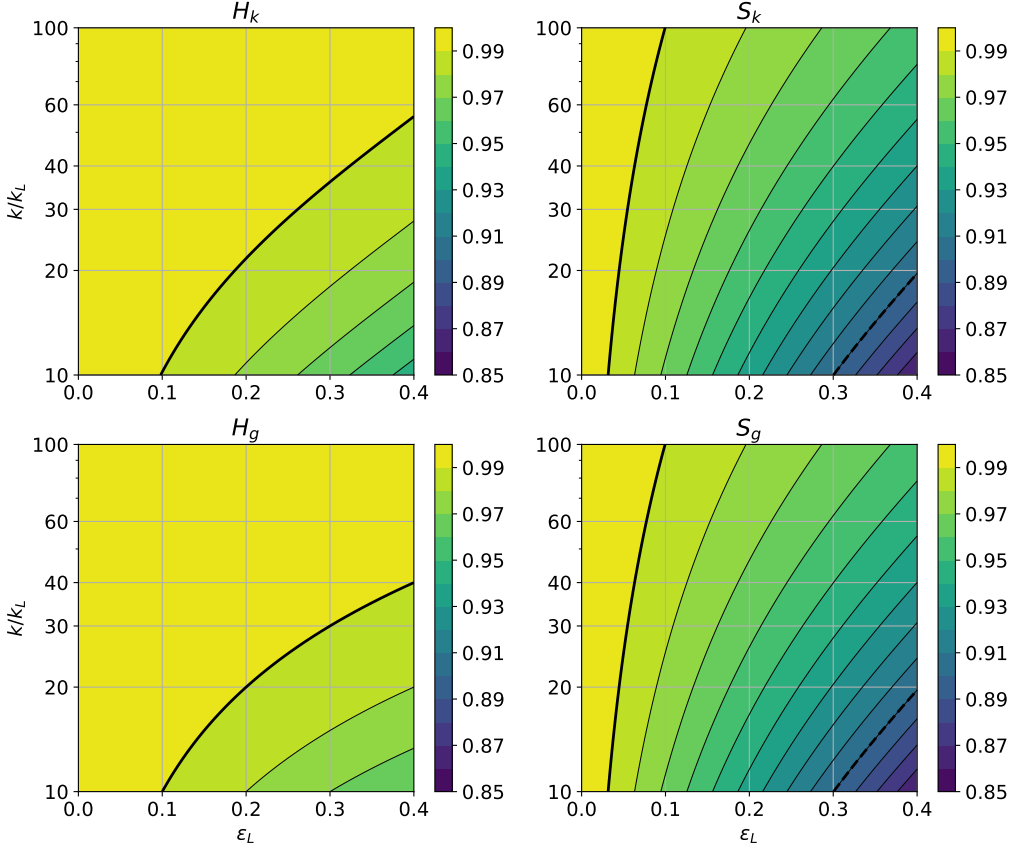


Figure 6: Homogeneity (left) and stationarity (right) of the short-wave wavenumber (top) and effective gravity (bottom) as a function of the long-wave steepness ε_L and the wavenumber ratio k/k_L , based on the linearised solutions (3.27-3.30). Solid and dashed lines highlight the 0.99 and 0.90 values, respectively.

$$S_{k,N} = 1 - \frac{\sigma_L}{\sigma} \left| \frac{\varepsilon_L \sin \psi}{(1 + \varepsilon_L \cos \psi) \sqrt{1 - \varepsilon_L^2 \cos^2 \psi}} \right| \quad (3.29)$$

$$S_g = 1 - \frac{\sigma_L}{\sigma} \left| \frac{\varepsilon_L \sin \psi}{(1 - \varepsilon_L \cos \psi) \sqrt{1 - \varepsilon_L^2 \cos^2 \psi}} \right| \quad (3.30)$$

The steady, linearised solutions thus depend on both the wavenumber ratio k_L/k (homogeneity) or the frequency ratio σ_L/σ (stationarity) and the long-wave steepness ε_L .

Fig. 6 shows the homogeneities and stationarities of the short-wave wavenumber and effective gravity based on the steady solutions and their derived criteria as minima of (3.19)-(3.20). Stationarity is a stronger requirement than homogeneity. At the lowest scale separation considered ($k/k_L = 10$), short-wave wavenumber, action, and effective gravity are all strongly homogeneous ($H_{k,N,g} > 0.99$) for $\varepsilon_L < 0.1$. However, the solutions are only strongly stationary ($S_{k,N,g} > 0.99$) at a high scale separation of $k/k_L = 100$ for $\varepsilon_L < 0.1$.

If we consider weakly stationary conditions as $S_{k,N,g} > 0.9$, then the solutions satisfy the requirements for the wave action conservation for $\varepsilon_L < 0.3$ at $k/k_L = 10$, and for $\varepsilon_L < 0.4$ at $k/k_L > 20$. Although Bretherton & Garrett (1968) state that the wave action balance is valid to $O(k_L/k)$, applying the general criteria (3.19)-(3.20) yields an error of $O(\varepsilon_L k_L/k)$. We will revisit these criteria based on the numerical solutions of nonlinear wave action and crest conservation equations in the next section.

4. Numerical solutions

4.1. Model description

To quantify the contribution of the nonlinear terms in (2.5) and (2.6), and to evaluate the steadiness assumption of the analytical solutions, we now proceed to numerically integrate the full set of crest and action conservation equations. (2.5) and (2.6) are discretised using second-order central finite difference in space and integrated in time using the fourth-order Runge-Kutta method (Butcher & Wanner 1996). The space is divided into 128 grid points. This is effectively the same equation set and numerical configuration as that of Peureux *et al.* (2021), except that their long-wave orbital velocities are evaluated at $z = 0$ instead of $z = \eta_L$, thus neglecting the Stokes drift induced by long waves on short-wave groups (Stokes 1847; van den Bremer & Breivik 2018; Monismith 2020). Their gravity modulation also does not consider the nonlinear, Lagrangian, or slope effects, however, this difference does not qualitatively affect the results. Another difference is the choice of the numerical scheme for spatial differences, which in their case is the more sophisticated MUSCL4 scheme (Kurganov & Tadmor 2000). Although the second-order central finite difference is not appropriate for many numerical problems, in our case it is sufficient because it is conservative and the fields that we compute derivatives of are smooth and continuous. The maximum relative error of the centred finite difference in this model is $\approx 0.066\%$. The wavenumber and wave action are conservative over time within $O(10^{-7})$ and $O(10^{-5})$ relative error, respectively. We show in the next subsection that our numerical solutions for infinite long-wave trains are qualitatively equivalent to those of Peureux *et al.* (2021).

The numerical equations here are integrated in a fixed reference frame with periodic boundary conditions, rather than that moving with the long-wave phase speed. Either approach produces equivalent modulation results, however a fixed reference frame allows for a more intuitive interpretation of the results. This difference is important to keep in mind when comparing the results of Peureux *et al.* (2021) and those presented here; in their Fig. 1 the long-wave phase is fixed and the short waves are moving leftward with the speed of $C_{pL} - C_g - U$ (neglecting group speed inhomogeneity), whereas in the figures that follow, the long wave is moving rightward with its phase speed C_{pL} and the short waves (that is, their action) are moving rightward with the speed of $C_g + U$ (neglecting group speed inhomogeneity). The crest and action conservation equations are integrated in the curvilinear coordinate system in which the horizontal coordinate follows the long-wave surface, akin to Zhang & Melville (1990).

4.2. Comparison with analytical solutions

The first set of simulations is performed for the long-wave steepness of $\varepsilon_L = 0.1, 0.2$, and 0.4 (Fig. 7). The long-waves are initialised from rest ($a_L = 0$) and gradually ramped up to their target steepness over 5 long-wave periods to allow for a gentle increase of the long-wave forcing on the short waves (the importance of which we discuss in more detail in the next subsection). At $\varepsilon_L = 0.1$, the numerical solutions for the wavenumber, amplitude, and steepness modulation are all remarkably similar to the analytical solutions (Fig. 7a,d,g).

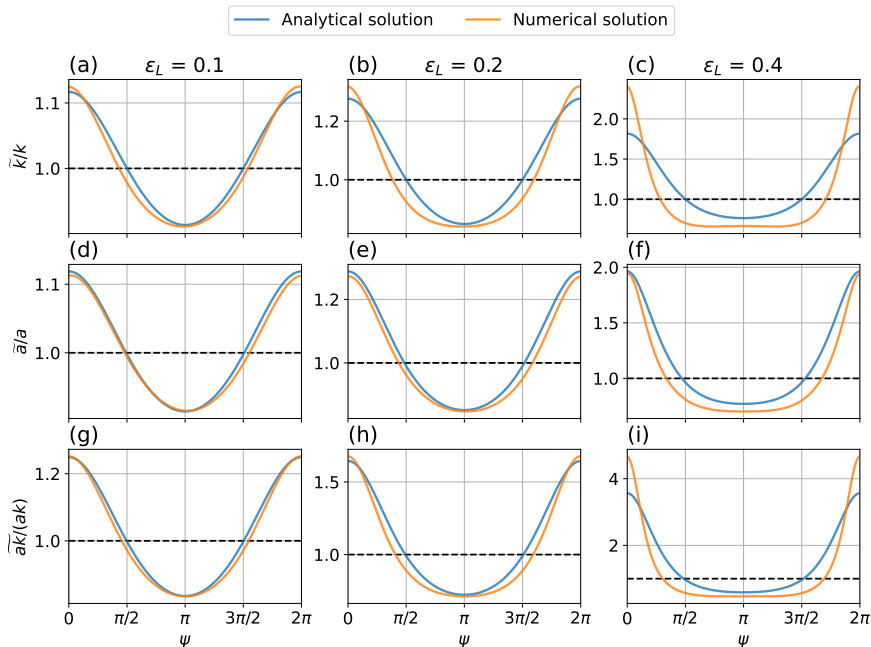


Figure 7: Comparison of numerical solutions (orange) of wavenumber (top), amplitude (middle), and steepness (bottom) modulation with their analytical solutions (blue), for $\varepsilon_L = 0.1, 0.2, \text{ and } 0.4$.

This suggests that for low ε_L the steady analytical solution is a reasonable approximation for the nonlinear crest-action solutions. The numerical solutions diverge more notably from the analytical ones at moderate $\varepsilon_L = 0.2$ (Fig. 7b,e,h), and are considerably different at very high $\varepsilon_L = 0.4$ (Fig. 7c,f,i). These differences suggest that at high ε_L the inhomogeneity of gravitational acceleration and group speed, otherwise ignored in the steady solutions, become important.

The maximum modulations of the short-wave wavenumber, amplitude, and steepness from the analytical and numerical solutions, are shown on Figs. 8, 9, and 10, respectively, as function of the long-wave steepness ε_L . Overall, the numerical solutions, based on the linear and the third-order Stokes long waves alike, begin to diverge from the analytical solution at $\varepsilon_L \approx 0.15$. The numerical solution using the third-order Stokes long wave is quantitatively very similar to the fully-nonlinear solutions of Longuet-Higgins (1987) in wavenumber modulation, however with somewhat lower amplitude and steepness modulations. Using the velocity and gravity properties of a fully-nonlinear wave, based on the approach by Clamond & Dutykh (2018), the numerical solutions diverge from those of the third-order Stokes wave only at very large steepnesses ($\varepsilon_L > 0.3$). Using a fully-nonlinear form of the long-wave thus does not collapse the difference between the solutions here and those of Longuet-Higgins (1987). For example, at $\varepsilon_L = 0.4$, the steepness modulation in our solution is 6.6, whereas Longuet-Higgins (1987) finds it to be 7.8. A possible reason for this difference is that the solutions by Longuet-Higgins (1987) are stationary (see his §2), whereas in our numerical model we solve the prognostic nonlinear equations for the short-wave wavenumber and action. As we will see in the next section, and as was suggested by Peureux *et al.* (2021), they are often, but not always, mostly steady, and can be strongly unsteady in special cases. Nevertheless, the overall steepness modulation between the two numerical approaches are

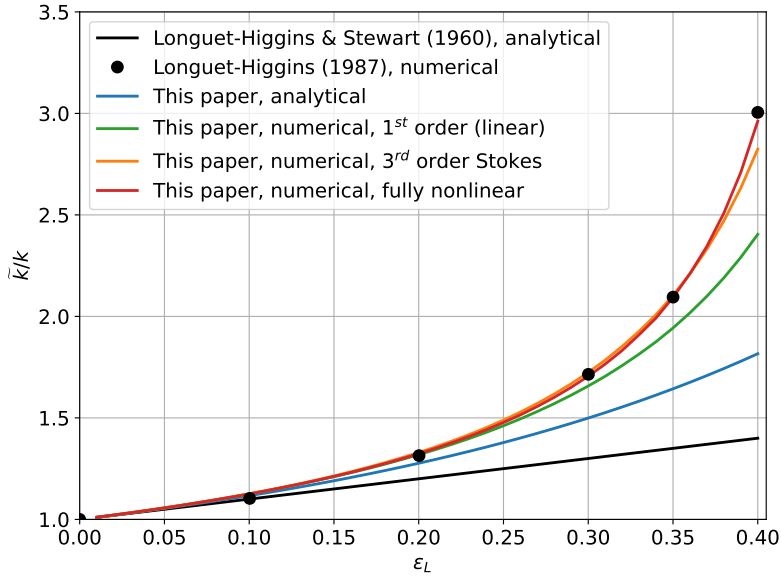


Figure 8: Maximum wavenumber modulation as function of long-wave steepness ε_L . Black line and circles are for the analytical and numerical solutions from Longuet-Higgins & Stewart (1960) and Longuet-Higgins (1987), respectively. Blue line is based on the analytical solutions from this paper. Green and orange lines are for the numerical solutions from this paper using linear and third-order Stokes approximations of long waves, respectively. Red line is for the fully-nonlinear gravity wave based on Clamond & Dutykh (2018).

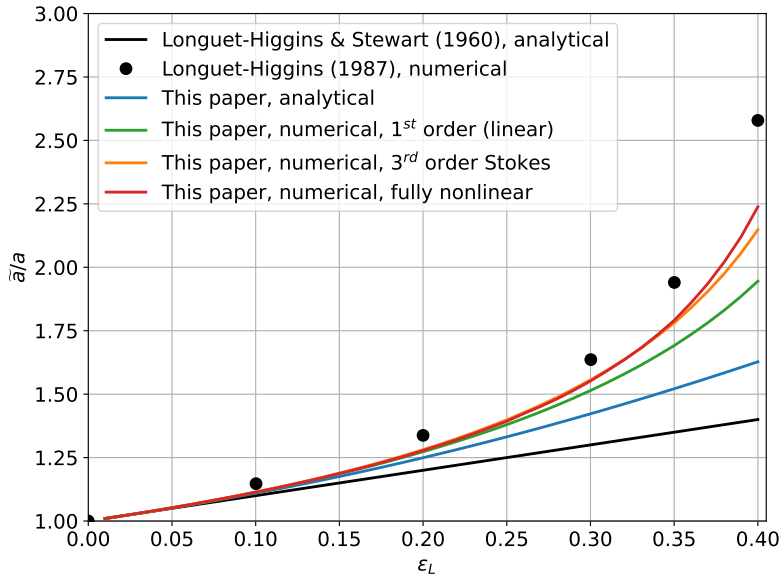


Figure 9: As Fig. 8 but for the amplitude modulation.

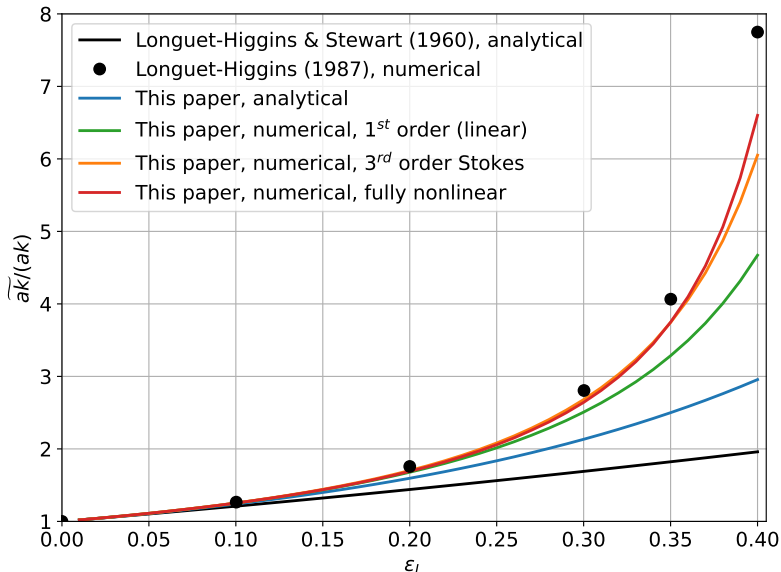


Figure 10: As Fig. 8 but for the steepness modulation.

remarkably similar, and either solution would cause the short-waves of moderate steepness to break (Banner & Peregrine 1993). Specifically, where the two modulation solutions differ ($\epsilon_L \gtrsim 0.3$), the steepness modulation approaches and exceeds 3. Tripling the short-wave steepness of even $\epsilon = 0.1$ would bring the wave train near the observed breaking thresholds of $\epsilon \gtrsim 0.32$ (Perlin *et al.* 2013), although, recent measurements show evidence of significantly higher breaking thresholds (Toffoli *et al.* 2010; McAllister *et al.* 2024), and even exceeding the geometric Stokes limit of 0.44. Nevertheless, in the cases where the short-waves would survive the modulation and persist over multiple long-wave periods, the two solutions are effectively equivalent.

As the numerical solutions are for the nonlinear wave action and crest conservation equations, it is important to re-evaluate the homogeneity and stationarity requirements for the wave action conservation to remain valid. Fig. 11 shows the homogeneities and stationarities of the short-wave wavenumber, action, and effective gravity as function of the long-wave steepness ϵ_L and the wavenumber ratio k/k_L , based on the numerical simulations. Although homogeneity is slightly lower ($H_{k,N,g} \approx 0.92$ for $k/k_L = 10$ and $\epsilon_L = 0.4$) compared to the analytical solutions, the stationarity is significantly reduced. Following the same criteria for strong ($S_{k,N,g} > 0.99$) and weak ($S_{k,N,g} > 0.9$) stationarity as in §3.4, the numerical solutions are only weakly stationary for $\epsilon_L < 0.21$ at $k/k_L = 10$, and for $\epsilon_L < 0.36$ at $k/k_L = 100$. This provides a quantitative guidance on when the short-wave action can be considered to be conserved in the presence of longer waves.

4.3. Unsteady growth in Pereux *et al.* (2021)

The key result of Peureux *et al.* (2021) is that of unsteady steepening of short waves when a homogeneous field of short waves is forced by an infinite long-wave train. The steepening is driven by the progressive increase in the action of short waves (as opposed to their wavenumber), and is centred on the short-wave group that begins its journey in the trough of the long wave. This is because the unmodulated short waves that begin their journey in the trough first enter the convergence region before reaching the divergence region. Inversely, the

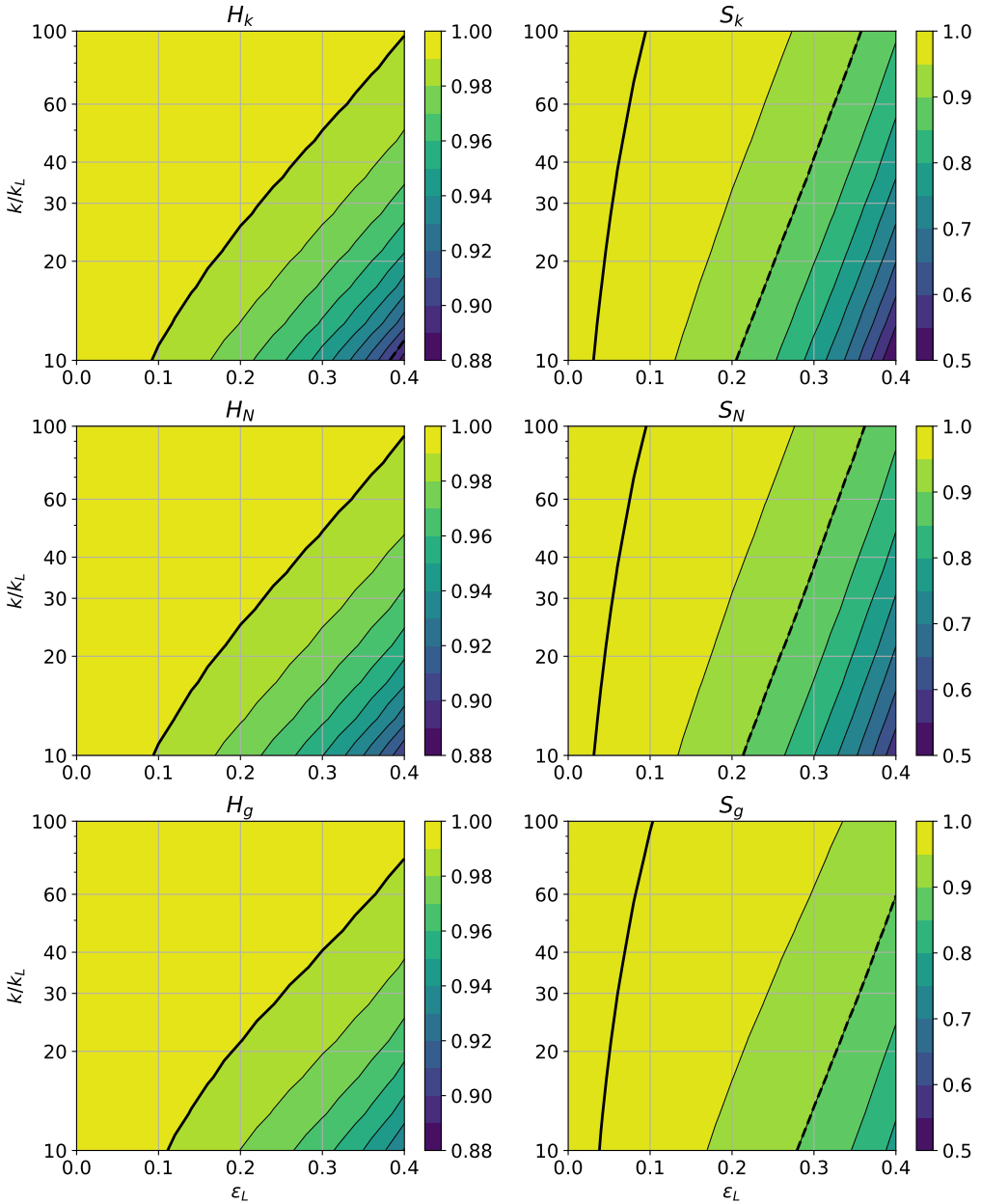


Figure 11: Homogeneity (left) and stationarity (right) of the short-wave wavenumber (top), action (middle), and effective gravity (bottom) as a function of the long-wave steepness ε_L and the wavenumber ratio k/k_L , based on the numerical solutions of the full wave crest and action conservation equations. Note that the color ranges are different than those in Fig. 6.

short waves that begin around the crest of the long-wave first enter the divergence region and will thus have their action and wavenumber decreased. We reproduce this behaviour in Fig. 12, which shows the evolution of the short-wave action, wavenumber, and steepness modulation (here defined as the change of a quantity relative to its initial value). The long waves have $\varepsilon_L =$

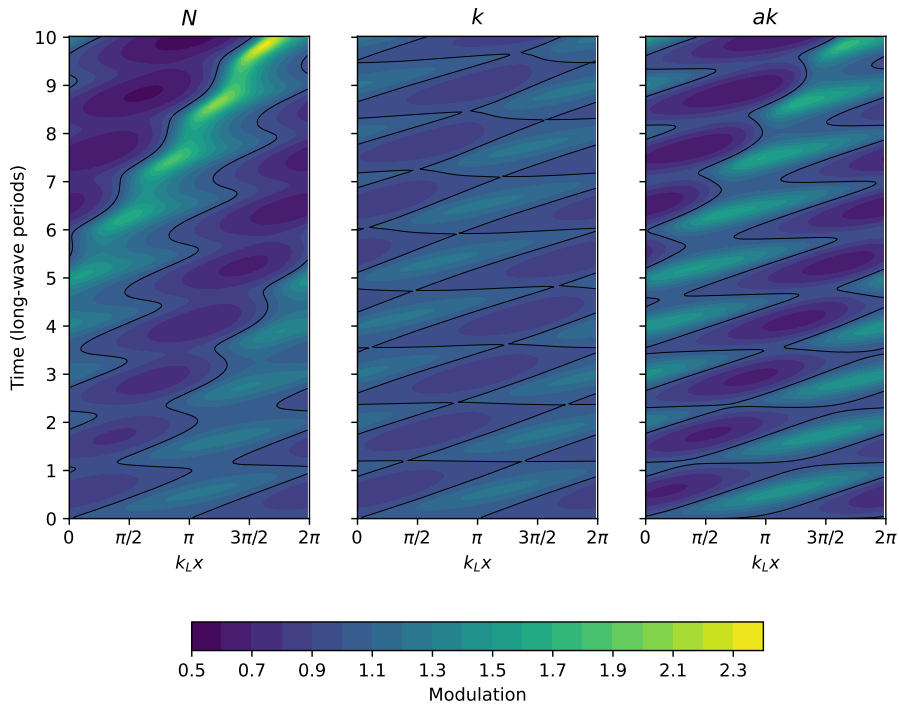


Figure 12: Change in the short-wave action (left), wavenumber (middle), and steepness (right) relative to their initial values as function of initial long-wave phase and time. $k_L = 1$, $k = 10$, $\varepsilon_L = 0.1$. The black contour follows the value of 1, which corresponds to no change from the initial values.

0.1 and $k_L = 1$, and the short waves have $k = 10$. After 10 long-wave periods, the short-wave action is approximately doubled, consistent with Peureux *et al.* (2021). Another important property of this solution is that the short-wave group that experiences peak amplification (attenuation) are not locked-in to the long-wave crests (troughs), as they are in the prior steady solutions (Longuet-Higgins & Stewart 1960; Longuet-Higgins 1987; Zhang & Melville 1990).

Why does this unsteady growth of short-wave action occur? Peureux *et al.* (2021) explain that the change in advection velocity due to the modulation of the short-wave group speed yields an additional amplification of the short-wave action. That is, the inhomogeneity term $N\partial C_g/\partial x$ is responsible for the instability. However, the instability only occurs if the short waves are initialised as a uniform field. If they are initialised instead as a periodic function of the long-wave phase such that their wavenumber (and optionally, action) is higher on the crests and lower in the troughs, akin to the prior steady solutions, the instability vanishes and the short-wave modulation pattern locks-in to the long-wave crests.

Why is it, then, that the solution for short-wave modulation is not only quantitatively, but also qualitatively, different depending on the short-wave initial conditions? It may at first seem that there is something special about the uniform initial conditions that makes its solutions grow unsteadily and indefinitely. Peureux *et al.* (2021) described this scenario as "...the sudden appearance of a long wave perturbation in the middle of a homogeneous short wave field". However, it is not obvious whether such a scenario is common as waves tend to

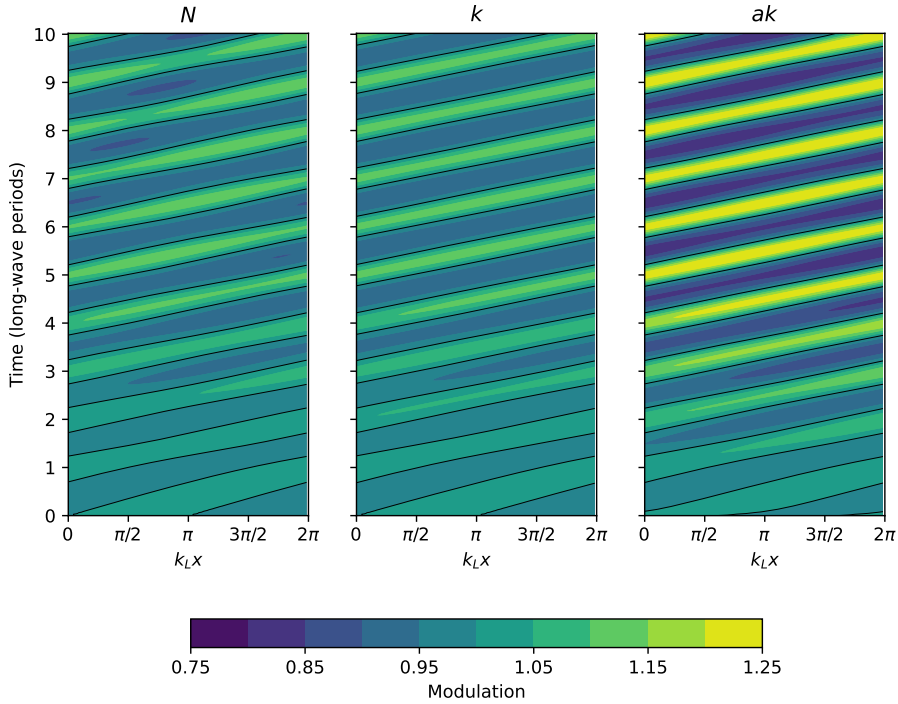


Figure 13: Same as Fig. 12 but with a linear ramp applied to a_L during the initial five long-wave periods. Notice the change in the colour range.

disperse into groups, and the time scales of incoming swell fronts are much longer than those of short-wave generation by wind. Exceptional situations with such a sudden onset of swell may occur around complex coastlines or in shadows behind islands, where wind-generated ripples may propagate from an otherwise calm sea state into the path of a crossing swell. Within the limits of the modulation theory used here, such short waves could quickly steepen and break.

To test whether the sudden onset of long-wave forcing causes the unsteady growth, we repeat the numerical simulation of Fig. 12, except for a linear ramp applied to a_L (and consequently, the other long-wave properties including the orbital velocities and the local steepness) for the first five periods: $a_L(t) = \min(a_L, a_L t / (5T_L))$, where T_L is the long-wave period. This result is shown in Fig. 13. Note that the linear ramp is strictly a numerical modeling technique to test the sensitivity of the solution to the sudden forcing at the beginning of the simulation, and is not intended to represent a physical process. The key distinction that arises with the introduction of the ramp is that the modulation pattern of short waves is now locked-in to the long-wave crests, and their indefinite steepening vanishes. The stabilisation effect of the long-wave ramp is more readily assessed in Fig. 14, which shows the maximum short-wave steepness modulation as function of time over 30 long-wave periods, for the infinite long-wave train case and the case of applying a linear ramp. Comparing the wave action propagation ($C_g \partial N / \partial x$) and inhomogeneity ($N \partial C_g / \partial x$) tendencies reveals that after only one long-wave period, the propagation and inhomogeneity tendencies are unbalanced and amplify the steepening of short waves (Fig. 15). Peureux *et al.* (2021) correctly pointed out that the unsteady growth of short-wave steepness occurs due to the resonance of the

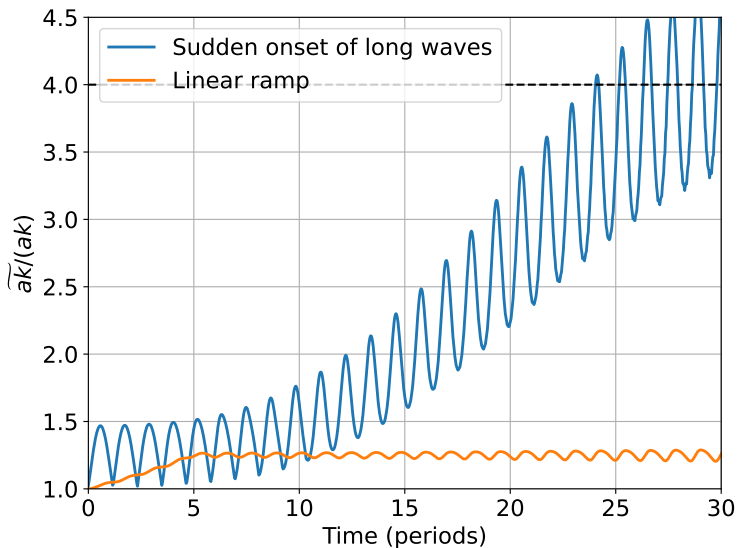


Figure 14: Maximum short-wave steepness modulation as function of time in case of infinite long-wave train case (blue) and the same case but with a linear ramp during the initial five long-wave periods (orange). The dashed black line corresponds to the short-wave steepness of 0.4 at which most waves are expected to break.

inhomogeneity tendency with the short-wave action perturbation. However, in the case of a gentle ramp-up of the long-wave forcing, the propagation and inhomogeneity tendencies balance each other and allow the short-wave steepening to lock-in to the long-wave crests.

4.4. Modulation by long waves of varying amplitude

We now proceed to examine the numerical solutions of short-wave modulation by long waves whose amplitude varies with time. The amplitude variation aims to mimic the behaviour of long-wave groups, a phenomenon that is ubiquitous in the ocean due to the dispersive nature of surface gravity waves, as well as due to the fact that wind-generated waves evolve to have broad-banded spectra. For simplicity of implementation and interpretation, the wave group here is simulated as a non-dispersive train of long waves whose amplitude scales with $\sin[\pi t/(nT_L)]$, where n is the number of long waves in the group. The elevation of the long waves thus gradually ramps up from rest to a_L at $t = nT_L/2$, after which it gradually decreases toward zero. In this simulation, $k/k_L = 10$ and $\varepsilon_L = 0.1$ as in the previous two simulations. The modulations of short-wave wavenumber, amplitude, and steepness in response to such long-wave group is shown in Fig. 16. Like in the case of a linear ramp, the modulation pattern here is locked in to the long-wave crest and peaks at approximately 1.2 for short-wave steepness of 0.1. After the peak of the long-wave group passes, the short-wave modulation recedes back toward the resting state.

5. Discussion

The solutions presented here, analytical and numerical alike, are valid only for certain scales of short and long waves. Specifically, the wave action conservation equation, introduced by Bretherton & Garrett (1968), requires that the ambient velocity is slowly varying on the time

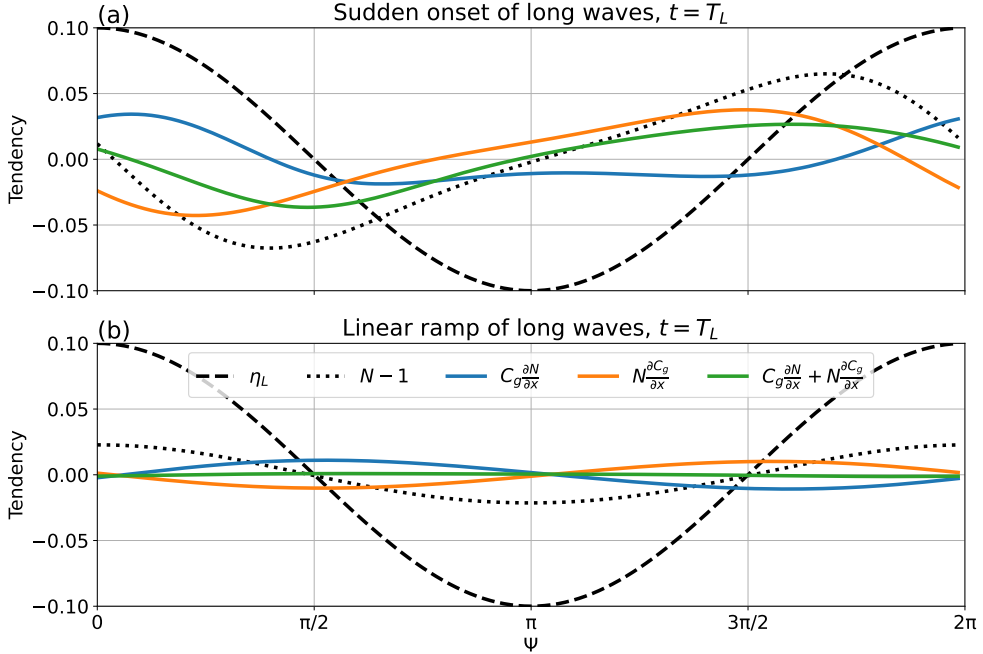


Figure 15: Propagation ($C_g \frac{\partial N}{\partial x}$) (blue) and inhomogeneity ($N \frac{\partial C_g}{\partial x}$) (orange) tendencies and their sum (green) for the short-wave action after one long-wave period, in the case of (a) infinite long-wave train and (b) linear ramp of long-wave amplitude. Dashed line is the long-wave elevation and the dotted line is the short-wave action modulation minus 1.

scales of short waves, *i.e.* $|\partial U/\partial x| \ll k|U|$ and $|\partial U/\partial t| \ll \sigma|U|$. This implies $k_L \ll k$ and $\sigma_L \ll \sigma$, respectively. The same requirement is imposed on the properties of short waves, including wavenumber, amplitude, and effective gravity. Another requirement is for the short-waves to remain linear, which implies $ak \ll 1$. These requirements have been evaluated for the solutions presented here by quantifying the homogeneity and stationarity of each relevant property of the flow in §3.4. Furthermore, the short waves examined here do not include the effects of surface tension (gravity-capillary waves) or intermediate or shallow water, although the solutions can be extended to those conditions, as Phillips (1981) did, for example. Within these limits, the crest-action conservation equations provide an elegant and simple framework to study the hydrodynamic modulation of short waves by longer waves. This approach, of course, isolates this particular process from other dominant modulation and nonlinear transfer processes, such as wave growth by wind, wave dissipation, and aerodynamic sheltering by the longer waves, that are otherwise present in most measurements (e.g., Plant 1986; Laxague *et al.* 2017). An alternative approach using a fully-nonlinear velocity potential flow solver that allows for two-way interaction between short and long waves would provide additional insight into the modulation of the long waves by the short waves.

Although in this paper we only explored the solutions for $k_L = 1$ and $k = 10$ the results are not sensitive to different values of k_L , provided the same long-wave steepness $\varepsilon_L = a_L k_L$. Numerical simulations with $k/k_L = 10$ and $k/k_L = 100$ show little sensitivity to the ratio k/k_L (not shown), consistent with the results of Longuet-Higgins (1987). Specifically, the short-wave steepness modulation is 1% larger at $\varepsilon_L = 0.27$ for $k/k_L = 10$ compared to $k/k_L = 100$, and 4% larger at $\varepsilon_L = 0.4$. This suggests that as long as $k/k_L \gg 1$, the modulation amplitude is largely independent of the ratio k/k_L . These results can be

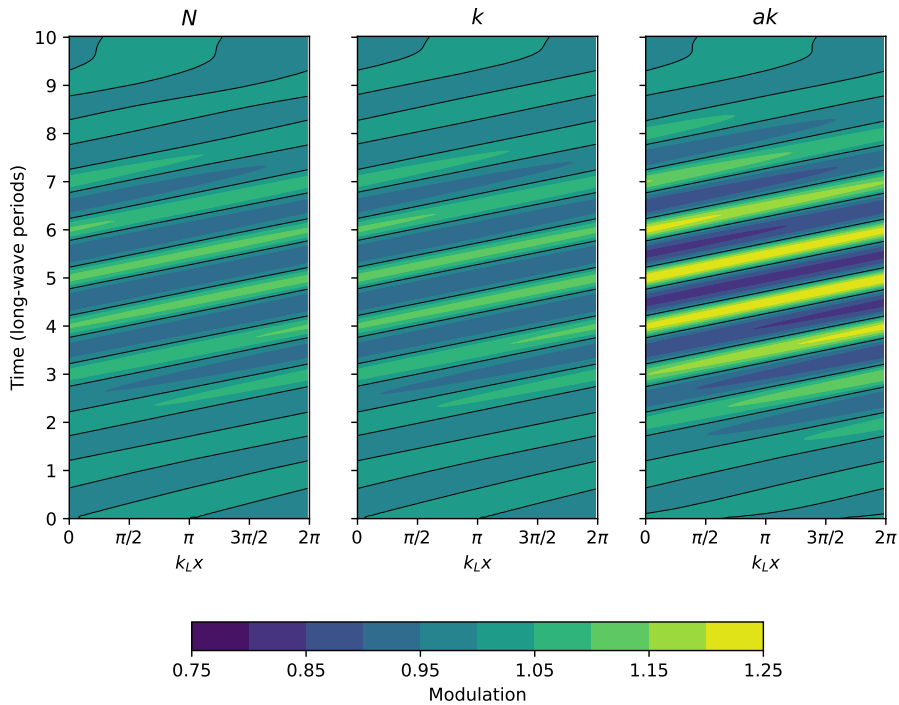


Figure 16: Same as Fig. 12 but for a long-wave group, causing the long-wave amplitude to gradually increase and peak at $a_L = 0.1$ after five long-wave periods, and then conversely decay back to a calm sea state.

reproduced with the companion numerical model. Note, however, according to §3.4, that the wave action conservation requirements are more easily satisfied for larger k/k_L . Also not considered here are the short-wave trains that are oblique to the longer waves, which is relatively straightforward to include (Peureux *et al.* 2021).

Despite several studies that provided qualitatively similar steady solutions for the short-wave modulation by long waves (Longuet-Higgins & Stewart 1960; Phillips 1981; Longuet-Higgins 1987; Henyey *et al.* 1988; Zhang & Melville 1990), it was not obvious from the governing prognostic equations that the steady solutions should exist generally. Peureux *et al.* (2021) examined this problem numerically and found that the solutions are stable only if the short-wave field is initialised from a prior steady solution of the form of that from Longuet-Higgins & Stewart (1960). If the short-wave field is instead initialised from a uniform field, they found that the short-wave amplitude, and thus steepness as well, grow unsteadily and indefinitely. Here we demonstrate that the unsteady steepening of short waves only occurs in the case of a sudden appearance of long waves, where the velocity fields induced by the long waves act in their full capacity on the short waves that have not yet had time to lock-in to the long-wave crests. In such a scenario, sudden forcing on short waves causes the modulation pattern to detach itself from the long-wave crests and to propagate at the short-wave group speed. When this occurs, the modulated short-waves are no longer in a stabilising resonance with the surface convergence and divergence induced by the long-wave orbital velocity, and each long-wave passage further destabilises the short-wave field, causing it to steepen indefinitely.

Another important consideration of the hydrodynamic modulation process is whether it should be accounted for in phase-averaged spectral wave models (WAMDI Group 1988; Tolman 1991; Donelan *et al.* 2012) used for global and regional wave forecasting. Second-order wave spectra have historically been provided by some wave models due to the importance for understanding radar altimetry data, however only in a diagnostic capacity (e.g., Janssen 2009). The framework by Janssen (2009), based on the Hamiltonian and the action series expansion by Zakharov (1968), is an alternative and more general approach to nonlinear wave evolution than the one described here. Currently, most spectral wave models used for research or forecasting do not consider the preferential steepening of short waves in the context of their dispersion properties or the wind input via the short-wave phase speed. Some dissipation source functions use the cumulative mean squared slope to quantify preferential dissipation of short waves due to this effect (Donelan *et al.* 2012; Romero 2019). In the early days of spectral wave modelling, Willebrand (1975) examined the effect of a wave spectrum on the short-wave group velocity and found the modulation effect to be up to several percent. For a practical implementation, this would incur an additional loop over all frequencies longer than the considered short-wave frequency. It was thus not deemed practical to include this effect in wave models at the time. However, with the recent advances in computing power, machine learning for acceleration of complex functions, and phase-resolved modelling of short waves, considering the effect of wave-modulation beyond the simple cumulative mean squared slope deserves re-examination.

6. Conclusions

In this paper we revisited the problem of short-wave modulation by long waves from a wave action conservation perspective. Using the linearised wave crest and action conservation equations coupled with nonlinear solutions for the effective gravity, we derived steady, nonlinear, analytical solutions for the modulation of short wave wavenumber, amplitude, steepness, intrinsic frequency, and phase speed. The latter two were previously examined in the context of short-wave modulation (Longuet-Higgins 1962; Longuet-Higgins & Phillips 1962), and may be important for correctly calculating the wind input into short waves, which is proportional to the wind speed relative to the wave celerity. The approximate steady solutions yield higher wavenumber and amplitude modulation than that of Longuet-Higgins & Stewart (1960), and somewhat lower than the numerical solutions of Longuet-Higgins (1987) and Zhang & Melville (1990). This is mainly due to the analytical solution requiring the crest and action conservation equations to be linearised, and the nonlinearity arising due to the evaluation of short waves on the surface of the long wave (as opposed to the mean water level) and due to nonlinear effective gravity. In the steady solutions, the short-wave steepness modulation is dominated by the wavenumber modulation (5/8), followed by the wave action modulation (1/4), and is least affected by the effective gravity modulation (1/8). The homogeneity and stationarity criteria for wave action conservation are evaluated for both the analytical and numerical solutions. The stationarity is a stronger criterion than homogeneity, and is found to be strongly satisfied (> 99% stationary) for very gently sloped waves and weakly satisfied (> 90% stationary) for steeper waves.

The numerical solutions of the full wave crest and action conservation equations are consistent with the analytical solutions for $\varepsilon_L \lesssim 0.2$, and are similar in magnitude to the numerical solutions of Longuet-Higgins (1987) and Zhang & Melville (1990). The simulations also reveal that the unsteady growth of the short-wave steepness reported by Peureux *et al.* (2021) is due to the sudden appearance of long waves in a homogeneous short-wave field, a scenario that is unlikely to be common in the open ocean. A more likely condition, such as that of long-wave groups, is only mildly destabilising for the short

waves. These results suggest that for the long-wave steepness $\varepsilon_L \lesssim 0.2$, the analytical steady solutions presented here are sufficient to describe the modulation of short waves by long waves. For moderately steep long waves ($0.2 \lesssim \varepsilon_L \lesssim 0.3$), numerical solutions of non-linearised crest and action conservation equations are necessary to properly capture the short-wave steepness modulation. For steeper long waves ($\varepsilon_L \gtrsim 0.3$), the short-wave properties can no longer be considered stationary (Bretherton & Garrett 1968); the wave action conservation equation is thus not valid in this context. It may be worthwhile to revisit a more systematic inclusion of the hydrodynamic modulation effects in phase-averaged spectral wave models, beyond the simple cumulative mean squared slope for wave dissipation, but also for modulating the dispersion and wind input into short waves.

Acknowledgements. I am thankful to Nathan Laxague, Fabrice Ardhuin, Nick Pizzo, and Peisen Tan for fruitful discussions. I also thank three anonymous reviewers for their expertise that helped improve this paper.

Funding. Milan Curcic was partly supported by the National Science Foundation grant AGS-1745384, Transatlantic Research Partnership by the French Embassy in the United States and the FACE Foundation, and the Office of Naval Research grants N000142012102 (Coastal Land Air-Sea Interaction DRI) and N000142412598 (in collaboration with SASCWATCH: Study on Air-Sea Coupling with WAVes, Turbulence, and Clouds at High winds MURI).

Declaration of interests. The author reports no conflict of interest.

Data availability statement. The code to run the numerical simulations and generate the figures in this paper is available at <https://github.com/wavesgroup/wave-modulation-paper>. The numerical model is available as a standalone Python package at <https://github.com/wavesgroup/2wave>. A Python implementation of SSGW by Clamond & Dutykh (2018) is available at <https://github.com/wavesgroup/ssgw>.

Author ORCIDs. M. Curcic, <https://orcid.org/0000-0002-8822-7749>

Appendix A. Surface velocity errors

The long-wave induced velocities (2.7)-(2.9) are accurate to $O(\varepsilon_L^3)$ when evaluated at the mean water level. However, in this paper we depart from the mean water level and evaluate the velocities at the surface of the long wave. This introduces additional errors at $O(\varepsilon_L^2)$. To quantify this error exactly, we compare the velocities evaluated at the surface for a linear (small-amplitude) wave and a third-order Stokes wave, with the surface velocity of a fully-nonlinear wave (Fig. 17). The elevation and the surface velocity for the fully-nonlinear wave is calculated numerically using the method by Clamond & Dutykh (2018), which relies on Petviashvili’s iterations and in this case uses 2048 Fourier modes to represent the wave. Both the first-order and the third-order waves underestimate the surface velocity at the crest and in the trough, and overestimate it on the front and rear faces of the crest.

Maximum values of surface velocity errors for both the linear and the third-order Stokes wave asymptote to ε_L^3 for small ε_L (Fig. 18). However, they approach and exceed ε_L^2 at $\varepsilon_L \approx 0.3$ and beyond. Although the maximum error is $\approx 10 - 20\%$ smaller for the third-order Stokes wave relative to the linear wave, its average error is slightly larger. The main takeaway from this figure is that evaluating the surface velocity of a linear wave carries an error no greater than ε_L^2 for $\varepsilon_L < 0.32$. Field measurements of near-surface orbital velocities by Laxague & Zappa (2020) qualitatively support this result, although they find larger departures from the linear theory in stronger winds, that is, steeper waves.

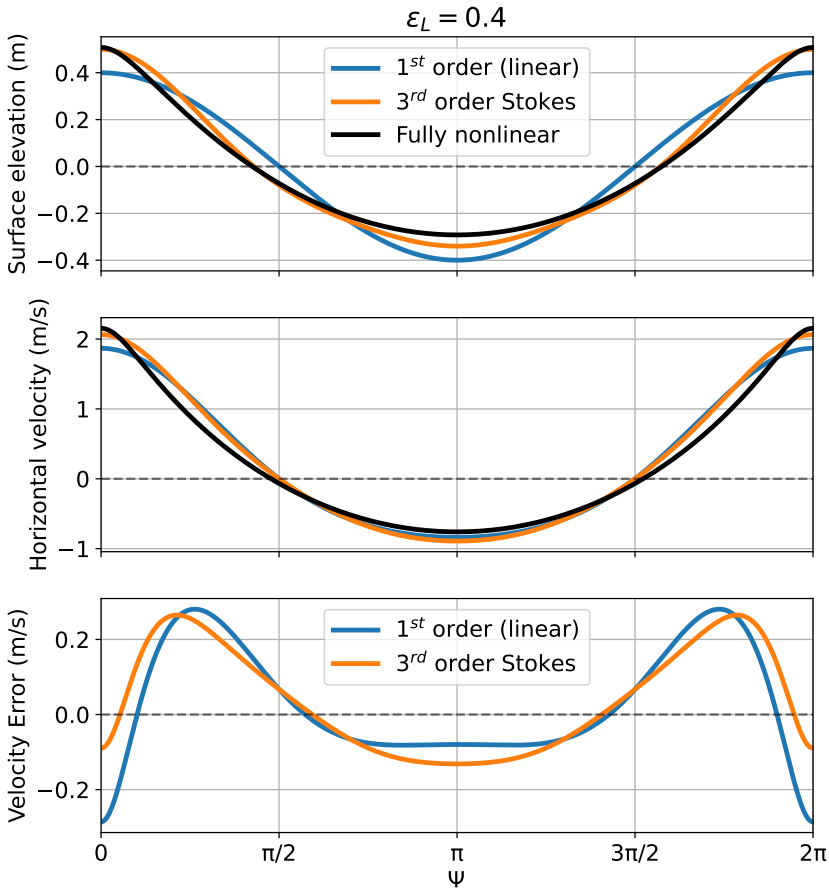


Figure 17: Surface elevation (top) and horizontal velocity (middle) for the linear wave (blue), the third-order Stokes wave (orange), and the fully-nonlinear wave (black) with steepness of $\varepsilon_L = 0.4$. The bottom panel shows the surface velocity error for the linear wave (blue) and the third-order Stokes wave (orange), relative to the fully-nonlinear wave solution.

- ALPERS, WERNER & HASSELMANN, KLAUS 1978 The two-frequency microwave technique for measuring ocean-wave spectra from an airplane or satellite. *Boundary-Layer Meteorology* **13**, 215–230.
- BANNER, ML & PEREGRINE, DH 1993 Wave breaking in deep water. *Annual review of fluid mechanics* **25** (1), 373–397.
- BELCHER, SE 1999 Wave growth by non-separated sheltering. *European Journal of Mechanics-B/Fluids* **18** (3), 447–462.
- VAN DEN BREMER, TON S & BREIVIK, ØYVIND 2018 Stokes drift. *Philosophical Transactions of the Royal Society A: Mathematical, Physical and Engineering Sciences* **376** (2111), 20170104.
- BRETHERTON, FRANCIS P & GARRETT, CHRISTOPHER JOHN RAYMOND 1968 Wavetrains in inhomogeneous moving media. *Proceedings of the Royal Society of London. Series A. Mathematical and Physical Sciences* **302** (1471), 529–554.
- BUTCHER, JOHN CHARLES & WANNER, GERHARD 1996 Runge-kutta methods: some historical notes. *Applied Numerical Mathematics* **22** (1-3), 113–151.

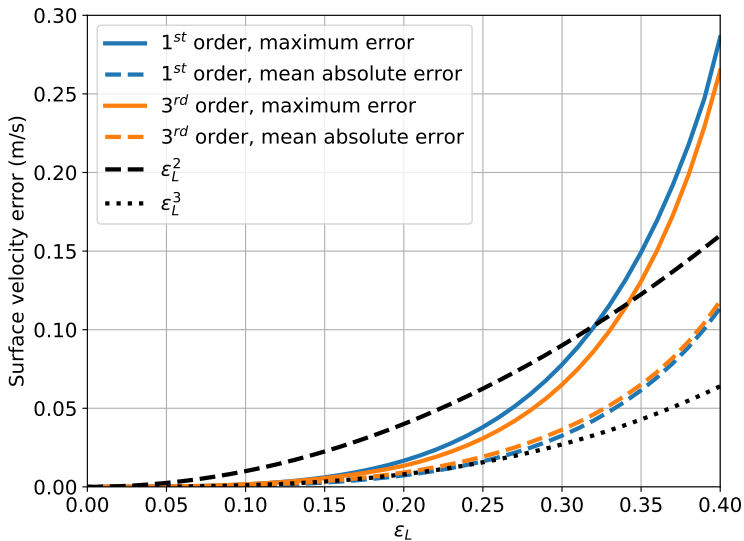


Figure 18: Surface velocity error as function of wave steepness ε_L , for the linear wave (blue) and the 3rd order Stokes wave (orange). Maximum and mean errors are indicated with solid and dashed lines, respectively. For reference, ε_L^2 and ε_L^3 curves are shown in black dashed and dotted lines, respectively.

- CHEN, GANG & BELCHER, STEPHEN E 2000 Effects of long waves on wind-generated waves. *Journal of Physical Oceanography* **30** (9), 2246–2256.
- CLAMOND, DIDIER & DUTYKH, DENYS 2018 Accurate fast computation of steady two-dimensional surface gravity waves in arbitrary depth. *Journal of Fluid Mechanics* **844**, 491–518.
- DONELAN, MA, CURCIC, M, CHEN, SS & MAGNUSON, AK 2012 Modeling waves and wind stress. *Journal of Geophysical Research: Oceans* **117** (C11).
- DONELAN, MARK A 1987 The effect of swell on the growth of wind waves. *Johns Hopkins APL Technical Digest* **8** (1), 18–23.
- DONELAN, MARK A, HAUS, BRIAN K, PLANT, WILLIAM J & TROIANOWSKI, OLIVIER 2010 Modulation of short wind waves by long waves. *Journal of Geophysical Research: Oceans* **115** (C10).
- DYSTHE, K, HENYEV, FS, LONGUET-HIGGINS, MICHAEL SELWYN & SCHULT, RL 1988 The orbiting double pendulum: an analogue to interacting gravity waves. *Proceedings of the Royal Society of London. A. Mathematical and Physical Sciences* **418** (1855), 281–299.
- HARA, TETSU, HANSON, KURT A, BOCK, ERIK J & UZ, B METE 2003 Observation of hydrodynamic modulation of gravity-capillary waves by dominant gravity waves. *Journal of Geophysical Research: Oceans* **108** (C2).
- HARA, TETSU & PLANT, WILLIAM J 1994 Hydrodynamic modulation of short wind-wave spectra by long waves and its measurement using microwave backscatter. *Journal of Geophysical Research: Oceans* **99** (C5), 9767–9784.
- HENYEV, FRANK S., CREAMER, DENNIS B., DYSTHE, KRISTIAN B., SCHULT, ROY L. & WRIGHT, JON A. 1988 The energy and action of small waves riding on large waves. *Journal of Fluid Mechanics* **189**, 443–462.
- JANSSEN, PETER AEM 2009 On some consequences of the canonical transformation in the hamiltonian theory of water waves. *Journal of Fluid Mechanics* **637**, 1–44.
- KELLER, WC & WRIGHT, JW 1975 Microwave scattering and the straining of wind-generated waves. *Radio science* **10** (2), 139–147.
- KURGANOV, ALEXANDER & TADMOR, EITAN 2000 New high-resolution central schemes for nonlinear conservation laws and convection–diffusion equations. *Journal of computational physics* **160** (1), 241–282.

- LAXAGUE, NATHAN JM, CURCIC, MILAN, BJÖRKQVIST, JAN-VICTOR & HAUS, BRIAN K 2017 Gravity-capillary wave spectral modulation by gravity waves. *IEEE Transactions on Geoscience and Remote Sensing* **55** (5), 2477–2485.
- LAXAGUE, NATHAN JM & ZAPPA, CHRISTOPHER J 2020 Observations of mean and wave orbital flows in the ocean's upper centimetres. *Journal of Fluid Mechanics* **887**, A10.
- LONGUET-HIGGINS, MS 1986 Eulerian and lagrangian aspects of surface waves. *Journal of Fluid Mechanics* **173**, 683–707.
- LONGUET-HIGGINS, MS 1987 The propagation of short surface waves on longer gravity waves. *Journal of Fluid Mechanics* **177**, 293–306.
- LONGUET-HIGGINS, MS & STEWART, RW 1960 Changes in the form of short gravity waves on long waves and tidal currents. *Journal of Fluid Mechanics* **8** (4), 565–583.
- LONGUET-HIGGINS, MICHAEL S 1962 Resonant interactions between two trains of gravity waves. *Journal of Fluid Mechanics* **12** (3), 321–332.
- LONGUET-HIGGINS, MICHAEL S & PHILLIPS, OWEN M 1962 Phase velocity effects in tertiary wave interactions. *Journal of Fluid Mechanics* **12** (3), 333–336.
- MCALLISTER, ML, DRAYCOTT, SAMUEL, CALVERT, R, DAVEY, T, DIAS, F & VAN DEN BREMER, TS 2024 Three-dimensional wave breaking. *Nature* **633** (8030), 601–607.
- MONISMITH, STEPHEN G 2020 Stokes drift: theory and experiments. *Journal of Fluid Mechanics* **884**, F1.
- PERLIN, MARC, CHOI, WOYOUNG & TIAN, ZHIGANG 2013 Breaking waves in deep and intermediate waters. *Annual review of fluid mechanics* **45** (1), 115–145.
- PEUREUX, CHARLES, ARDHUIN, FABRICE & GUIMARÃES, PEDRO VERAS 2021 On the unsteady steepening of short gravity waves near the crests of longer waves in the absence of generation or dissipation. *Journal of Geophysical Research: Oceans* **126** (1), e2020JC016735.
- PHILLIPS, OM 1981 The dispersion of short wavelets in the presence of a dominant long wave. *Journal of Fluid Mechanics* **107**, 465–485.
- PLANT, W 1977 Studies of backscattered sea return with a cw, dual-frequency, x-band radar. *IEEE Journal of Oceanic Engineering* **2** (1), 28–36.
- PLANT, WILLIAM J 1986 A two-scale model of short wind-generated waves and scatterometry. *Journal of Geophysical Research: Oceans* **91** (C9), 10735–10749.
- ROMERO, LEONEL 2019 Distribution of surface wave breaking fronts. *Geophysical Research Letters* **46** (17–18), 10463–10474.
- STEWART, ROBERT H & JOY, JOSEPH W 1974 Hf radio measurements of surface currents. In *Deep sea research and oceanographic abstracts*, , vol. 21, pp. 1039–1049. Elsevier.
- STOKES, GEORGE, G 1847 On the theory of oscillatory waves. *Transactions of the Cambridge Philosophical Society* **8**, 441–455.
- TOFFOLI, ALESSANDRO, BABANIN, ALEXANDER, ONORATO, MIGUEL & WASEDA, T 2010 Maximum steepness of oceanic waves: Field and laboratory experiments. *Geophysical Research Letters* **37** (5).
- TOLMAN, HENDRIK L 1991 A third-generation model for wind waves on slowly varying, unsteady, and inhomogeneous depths and currents. *Journal of Physical Oceanography* **21** (6), 782–797.
- UNNA, PJH 1941 White horses. *Nature* **148** (3747), 226–227.
- UNNA, PJH 1942 Waves and tidal streams. *Nature* **149** (3773), 219–220.
- UNNA, PJH 1947 Sea waves. *Nature* **159** (4033), 239–242.
- WAMDI GROUP 1988 The WAM model—A third generation ocean wave prediction model. *Journal of physical oceanography* **18** (12), 1775–1810.
- WHITHAM, GB 1965 A general approach to linear and non-linear dispersive waves using a lagrangian. *Journal of Fluid Mechanics* **22** (2), 273–283.
- WHITHAM, GB 1974 Dispersive waves and variational principles. *Nonlinear waves* pp. 139–169.
- WILLEBRAND, JÜRGEN 1975 Energy transport in a nonlinear and inhomogeneous random gravity wave field. *Journal of Fluid Mechanics* **70** (1), 113–126.
- ZAKHAROV, VLADIMIR E 1968 Stability of periodic waves of finite amplitude on the surface of a deep fluid. *Journal of Applied Mechanics and Technical Physics* **9** (2), 190–194.
- ZHANG, JUN & MELVILLE, WK 1990 Evolution of weakly nonlinear short waves riding on long gravity waves. *Journal of Fluid Mechanics* **214**, 321–346.